© 2016. Published by The Company of Biologists Ltd | Journal of Experimental Biology (2016) 219, 2311-2319 doi:10.1242/jeb.135566

RESEARCH ARTICLE

Intermuscular pressure between synergistic muscles correlates with muscle force

Lars Reinhardt[1,*], Tobias Siebert[2], Kay Leichsenring[3], Reinhard Blickhan[1] and Markus Böl[3]

ABSTRACT

The purpose of the study was to examine the relationship between muscle force generated during isometric contractions (i.e. at a constant muscle–tendon unit length) and the intermuscular (between adjacent muscles) pressure in synergistic muscles. Therefore, the pressure at the contact area of the gastrocnemius and plantaris muscle was measured synchronously to the force of the whole calf musculature in the rabbit species *Oryctolagus cuniculus*. Similar results were obtained when using a conductive pressure sensor, or a fibre-optic pressure transducer connected to a water-filled balloon. Both methods revealed a strong linear relationship between force and pressure in the ascending limb of the force-length relationship. The shape of the measured force–time and pressure–time traces was almost identical for each contraction (r=0.97). Intermuscular pressure ranged between 100 and 700 mbar (70,000 Pa) for forces up to 287 N. These pressures are similar to previous (intramuscular) recordings within skeletal muscles of different vertebrate species. Furthermore, our results suggest that the rise in intermuscular pressure during contraction may reduce the force production in muscle packages (compartments).

KEY WORDS: Muscle compression, Transversal muscle loading, Isometric contraction, Calf muscles, *Oryctolagus cuniculus*

INTRODUCTION

During contraction, most muscles predominantly produce forces in longitudinal direction, i.e. along a line from the origin to the insertion (McGinnis, 1999). Furthermore, the process of contraction entails changes in the muscle shape, e.g. increase in muscle thickness (Röhrle et al., 2008; Siebert et al., 2012; Böl et al., 2013, 2015; Wakeling et al., 2013). Because most muscles are tightly packed in muscle packages (compartments), these deformations may cause additional transverse forces (perpendicular to the line of action) in between contracting muscles or between muscles and surrounding tissues, e.g. bones or connective tissue. The strength of this interaction determines the amount of transverse compression. As a consequence, variations in the intermuscular pressure (IrMP), to be the pressure at the contact surfaces of the muscles, should occur.

According to recent studies, contraction dynamics are strongly influenced by unidirectional transversal muscle compression (Siebert et al., 2014a,b, 2016). Isometric experiments with and without transversal muscle loading (contact area: 0.5 cm^2) on rat M. gastrocnemius medialis demonstrated that, compared with an unloaded situation, the maximum isometric force and the rate of force development were reduced by 4.8% to 12.8% and 20.2% to 34.6%, respectively, at pressures ranging from 1.3 to 5.3 N cm^{-2} (Siebert et al., 2014b). Although these studies provided evidence that transversal muscle loading has an impact on contraction dynamics, only limited conclusions regarding the situation *in vivo* could be drawn. Particularly in the already mentioned muscle packages, it can be assumed that the pressure is distributed across a large proportion of the enveloping surface and not limited to a relatively small contact area only. Furthermore, the shape of muscles and connective tissue affects the pressure in between (Otten, 1988; van Leeuwen and Spoor, 1992) and a suitable shape may reduce the contact pressure.

Against this background, the question arises of whether the IrMP between adjacent muscles during contraction is in a relevant range to affect contractile function. A first indication on the answer is given by previous investigations on the intramuscular pressure (IaMP), i.e. the fluid pressure created by a muscle as it contracts within its fascial compartment. It has been known since the first attempts to characterise the mechanical properties of skeletal muscles (Hill, 1948) that they generate significant IaMP during active contraction. Furthermore, IaMP was reported to correlate linearly with contraction force in skeletal muscles of humans, cats and rabbits (Baskin and Paolini, 1967; Sadamoto et al., 1983; Parker et al., 1984; Petrofsky and Hendershot, 1984; Sejersted et al., 1984; Aratow et al., 1993; Nakhostine et al., 1993; Davis et al., 2003; Ward et al., 2007; Winters et al., 2009; Macias et al., 2012). According to present knowledge, muscle contraction causes a reversible distortion of muscle architecture accompanied by an increase of IaMP, owing to muscle incompressibility (Swammerdam, 1737; Hill, 1948; Jenkyn et al., 2002).

However, it was also found that the IaMP strongly depends on the measurement site, or, more precisely, pressure was higher the deeper the catheter was inserted (Sejersted et al., 1984; Nakhostine et al., 1993). Furthermore, owing to their simple accessibility, most studies were conducted on surface muscles like the M. tibialis anterior (TA) and not at the boundary areas of two muscles. Consequently, the existing intramuscular data can be transferred to the IrMP within muscle packages only to a limited extent.

In view of the need for additional experiments, methodological considerations have to be made. Whereas the microcapillary infusion technique was used in earlier investigations on IaMP determination (Styf and Körner, 1986), transducer-tipped semiconductor-based or fibre-optic-based catheter pressure sensors were used in more recent studies (Sondergaard et al., 2002; Kaufman et al., 2003; Cottler et al., 2009; Sezen et al., 2009). Because these methods require a fluid-filled space, which is non-existent between muscles, they are not suitable to measure the IrMP.

[1]Science of Motion, Friedrich-Schiller-University Jena, Seidelstr. 20, Jena D-07749, Germany. [2]Institute of Sport and Motion Science, University of Stuttgart, Allmandring 28, Stuttgart D-70569, Germany. [3]Institute of Solid Mechanics, Technical University Braunschweig, Schleinitzstr. 20, Braunschweig D-38106, Germany.

*Author for correspondence (lars.reinhardt@uni-jena.de)

L.R., 0000-0001-5054-5592

Received 27 November 2015; Accepted 16 May 2016

Journal of Experimental Biology (2016) 219, 2311-2319 doi:10.1242/jeb.135566

List of symbols and abbreviations

f	stimulation frequency
F	muscle force
F_{im}	maximum isometric force
GAS	Musculus gastrocnemius
IaMP	intramuscular pressure
IrMP	intermuscular pressure
l	muscle length (regarding the length at which muscle force was zero)
l_0	initial muscle–tendon unit length of the calf muscle package
l_{max}	muscle length at P_{max}
l_{opt}	muscle length at F_{im}
l_{PF}	muscle length for experiments with different stimulation frequencies
l_{reg}	maximum muscle length for regression analyses
M_b	body mass
MTU	muscle–tendon unit
n	number of trials
N	number of individuals
P	pressure
PLA	Musculus plantaris
P_{max}	maximum intermuscular pressure
SOL	Musculus soleus
TA	Musculus tibialis anterior

However, a fibre-optic sensor connected to a balloon catheter should be the method of choice (Tohyama et al., 1997). Furthermore, the application of a conductive polymer pressure sensor is conceivable as well (Ferguson-Pell et al., 2000). For this reason, both measurement methods were used in the present study.

In the rabbit calf, there are several muscles, such as M. soleus (SOL) and M. plantaris (PLA), that are almost completely surrounded by other muscles (Siebert et al., 2015). Recent studies measured prominent deformations of the three-dimensional muscle surface of SOL and PLA during isometric and dynamic muscle contraction (Böl et al., 2013, 2015). However, so far it is unclear to what extent these deformations induce transversal forces in between the muscles. Thus, the aim of the present study was to measure the IrMP between PLA and M. gastrocnemius (GAS) during isometric contractions with respect to active muscle force generation.

MATERIALS AND METHODS

The study was conducted on the basis of well-established methods and procedures to determine muscle properties and deformations that have already been described in detail (Böl et al., 2013, 2015; Siebert et al., 2015).

Animals and experimental setup

Six New Zealand white rabbits, *Oryctolagus cuniculus* (Linnaeus 1758), with an average body mass (M_b) of 3.49±0.66 kg (Table 1) were anaesthetised with bupivacain (Jenapharm®, 1 ml, 0.5%, epidural) after short-term sedation with natrium pentobarbital (Nembutal®, 80 mg kg^{-1} M_b). After removing the skin of the right hind leg below the knee, the rabbit was located in a fixation frame and fixed by three pairs of bone pins, at the hip, knee and ankle. Because muscle characteristics depend on temperature, the animals were kept on a constant temperature (39°C) during the entire experimental procedures using a heating pad (Harvard Apparatus, Holliston, MA, USA). Additionally, the calf surface was frequently sprinkled with heated (39°C) physiological saline solution during the entire experiment. Calf muscle packages, consisting of GAS, PLA and SOL, for the six rabbits were named CA1 to CA6, respectively. Experiments were approved according to Section 8 of the German animal protection law (Tierschutzgesetz, BGBl. I 1972, 1277).

Force measurements

In the used experimental set-up, the muscle–tendon unit (MTU) length was kept constant during the contractions. Although this is not valid at the level of the muscle fibre (see Discussion), we designate the experiments as isometric contractions throughout the paper.

A muscle lever (Model 310B-LR, Aurora Scientific Inc., Aurora, Ontario, Canada) was used to measure/generate length and force changes. The arm of the muscle lever was connected with a hook directly to the calcaneus to measure forces of SOL and GAS. The plantaris tendon was connected to the same lever arm via a metal clamp (Siebert et al., 2015). Muscle length of PLA was adjusted to reach maximum isometric force (F_{im}) at the same muscle-lever arm excursion as the other muscles. No interventions were made at the origins of the calf muscles.

At the beginning of all experiments, the initial length (l_0) of the calf-muscle package (114.0±5.2 mm) was measured *in situ* with a micrometre at an ankle joint angle of about 90 deg. To determine the force–length relationship of the calf muscles, isometric contractions (activation interval: 0.5–0.7 s; Fig. 2) were conducted with length increments of 2 mm. In these experiments, the muscle package was stimulated supramaximally (130 Hz) over the tibial nerve using a bipolar gold electrode. Rest intervals of 2 min were interposed between contractions to minimise fatigue effects. Passive muscle force was defined as the resting muscle force at each length and measured for each contraction bout during the 100 ms period prior to muscle stimulation. To ensure that the whole ascending limb of the force–length curve was recorded, measurements were repeated until the muscle force began to decrease.

Pressure measurements

In order to measure IrMP, two different transducer types were used: (1) a fibre-optic pressure-measurement system (Samba; Samba Sensors AB, Göteborg, Sweden) and (2) a conductive polymer pressure sensor (FlexiForce B201; Tekscan Inc., Boston, MA, USA). For the experiments that were conducted simultaneously to the force measurements, one of the two transducers was inserted from the medial and distal direction in the gap between the GAS and PLA. The transducer was pushed carefully in a proximal direction and positioned as centrally as possible between the contact area of the GAS and PLA (Fig. 1A,B). Pressure transducers were placed at the same position for each experiment, which was validated by photography.

The details of the Samba sensor (Sensor 1) were presented previously (Sondergaard et al., 2002). Because this sensor is designed for use in fluids and gases, we connected it to a small water-filled rubber balloon, which was positioned between the calf muscles (Fig. 1). Pilot studies inserting the sensor directly in between the muscles resulted in non-reproducible results owing to a lack of liquid. The balloon was fixed by a thread on the tip of an irrigation cannula from stainless steel. Luer-lock adapters were used to connect the cannula to a brass tube including the Samba sensor, and to vent or to fill the system with water, respectively. Signals of the Samba system were captured synchronously to the force data at 1000 Hz.

The dimensions (approximately 30 mm in length, 8 mm in width and 2.5 mm in depth) and fill volume (≈0.5 ml) of the balloon were chosen so that a large proportion of the contact area between the GAS and PLA was covered and in such a way that it was not possible

Journal of Experimental Biology (2016) 219, 2311-2319 doi:10.1242/jeb.135566

Table 1. Muscle parameters and results of the linear regression analyses given for the Samba (Sensor 1) and the FlexiForce (Sensor 2) sensors

	CA1	CA2	CA3	CA4	CA5	CA6	Mean	s.d.
Symbol	●	◆	★	■	▲	▼		
Body mass (kg)	4.34	2.52	2.94	3.63	3.86	3.65	3.49	0.66
Initial muscle length (mm)	123.6	111.5	111.3	111.3	110.0	116.3	114.0	5.2
Maximum stress (N cm^{-2})	17.9	15.7	16.3	13.1	12.8	12.5	14.7	2.0
Sensor 1								
Force–length relationship								
F_{im} (N)	284.9	186.0	194.9	180.0	198.8	182.9	204.6	40.0
l_{opt} (mm)	16.2	14.3	13.6	14.6	12.9	16.8	14.8	1.5
l_{reg} (mm)	14.2	10.3	11.6	12.6	12.9	12.8	12.4	1.3
$F(l)=a\cdot l$								
a (N mm^{-1})	19.0	15.7	15.8	13.4	15.7	12.7	15.4	2.2
r^2	0.997	0.992	0.998	0.996	0.997	0.994	0.996	0.002
Pressure–length relationship								
P_{max} (mbar)	700.9	457.2	396.8	544.3	650.9	484.2	539.0	117.2
l_{max} (mm)	16.2	10.3	11.6	8.6	10.9	8.8	11.1	2.8
l_{reg} (mm)	16.2	10.3	11.6	8.6	10.9	8.8	11.1	2.8
$P(l)=a\cdot l+b$								
a (mbar mm^{-1})	39.9	34.6	18.2	27.6	37.5	33.0	31.8	7.9
b (mbar)	34.9	127.7	184.2	320.5	245.9	206.1	186.5	98.3
r^2	0.973	0.980	0.997	0.955	0.999	0.988	0.982	0.004
Sensor 2								
Force–length relationship								
F_{im} (N)	287.4				217.9		252.6	49.3
l_{opt} (mm)	16.4				15.7		16.0	0.5
l_{reg} (mm)	14.4				11.7		13.0	1.9
$F(l)=a\cdot l$								
a (N mm^{-1})	19.2				16.7		17.9	1.8
r^2	0.996				0.995		0.996	0.001
Pressure–length relationship								
P_{max} (mbar)	697.2				561.8		629.5	95.7
l_{max} (mm)	14.4				11.7		13.0	1.9
l_{reg} (mm)	14.4				11.7		13.0	1.9
$P(l)=a\cdot l+b$								
a (mbar mm^{-1})	43.7				38.6		41.1	3.6
b (mbar)	28.6				82.0		55.3	37.8
r^2	0.968				0.973		0.970	0.003

l_{opt}, muscle length at F_{im}; l_{reg} and l_{max} are the maximum muscle length for regression analyses and muscle length at the maximum intermuscular pressure, respectively; F_{im}, maximum isometric force. Maximum muscle stress was calculated using muscle mass, optimal fibre length and muscle density of 1.056 g cm^{-3} (Mendez and Keys, 1960; Siebert et al., 2015).

to fully squeeze it at pressures up to 1 bar. Thus, by the use of this method, we determined the average pressure between both muscles without resolving local variations.

As a reference, in two of the animals (CA1 and CA5), we repeated our measurements with the FlexiForce sensor (Sensor 2). The suitability of this device for the measurement of interface pressures on biological tissues has already been proven (Ferguson-Pell et al., 2000). In order to avoid curvature effects [the reading of the sensor is affected by a curved surface (Ferguson-Pell et al., 2000)] and to concentrate the muscle pressure on a defined area, we equipped the sensing area (Ø 9.5 mm) with thin (0.5 mm) brass discs on its upper and lower side (Fig. 1C). The Tekscan Economical Load & Force (ELF™) system was used to sample the signals at 200 Hz.

All pressure values are given in the metric unit mbar (1 mbar=100 Pa=0.01 N cm^{-2}).

Variation of muscle force at constant muscle length by stimulation frequency

In order to elucidate whether IrMP depends on muscle force (F) rather than muscle length (l), we conducted experiments at the same MTU length but with different stimulation frequencies (f; from 20 Hz to 130 Hz). With this experimental setting, we altered the force without changing the muscle length. However, as the stimulation frequencies increased, the muscle fibres would have shortened as the tendons stretched owing to the higher forces.

Data analyses

All calculations were made in MATLAB R2013b (The MathWorks, Natick, MA, USA). Signals were smoothed using a moving average filter with a box width of 50 points. By this filter selection, the signal noise was effectively reduced without changing the characteristics of the trajectories. In accordance with previous findings, we assumed the ascending limb of the force–length relationship to be linear (Blix, 1894; Gordon et al., 1966; Siebert et al., 2015). Therefore, least-squares linear regressions were used to determine the relationships between muscle length, isometric force, and intermuscular pressure in the ascending limb. As a measure for the strength of the association, the coefficient of determination (r^2) was used. The criterion to exclude data points in the plateau region (unfilled symbols in Fig. 3) was to maximise r^2 for the linear regression of the ascending limb of the force–length relationship. Similarities of curve progressions were examined using Pearson's linear correlation coefficient (r). To improve comparability of the force–length relationships, all curves were shifted to the length at the ascending limb of the force–length relationships at which the muscle force was zero. This length was defined as zero muscle

Journal of Experimental Biology (2016) 219, 2311-2319 doi:10.1242/jeb.135566

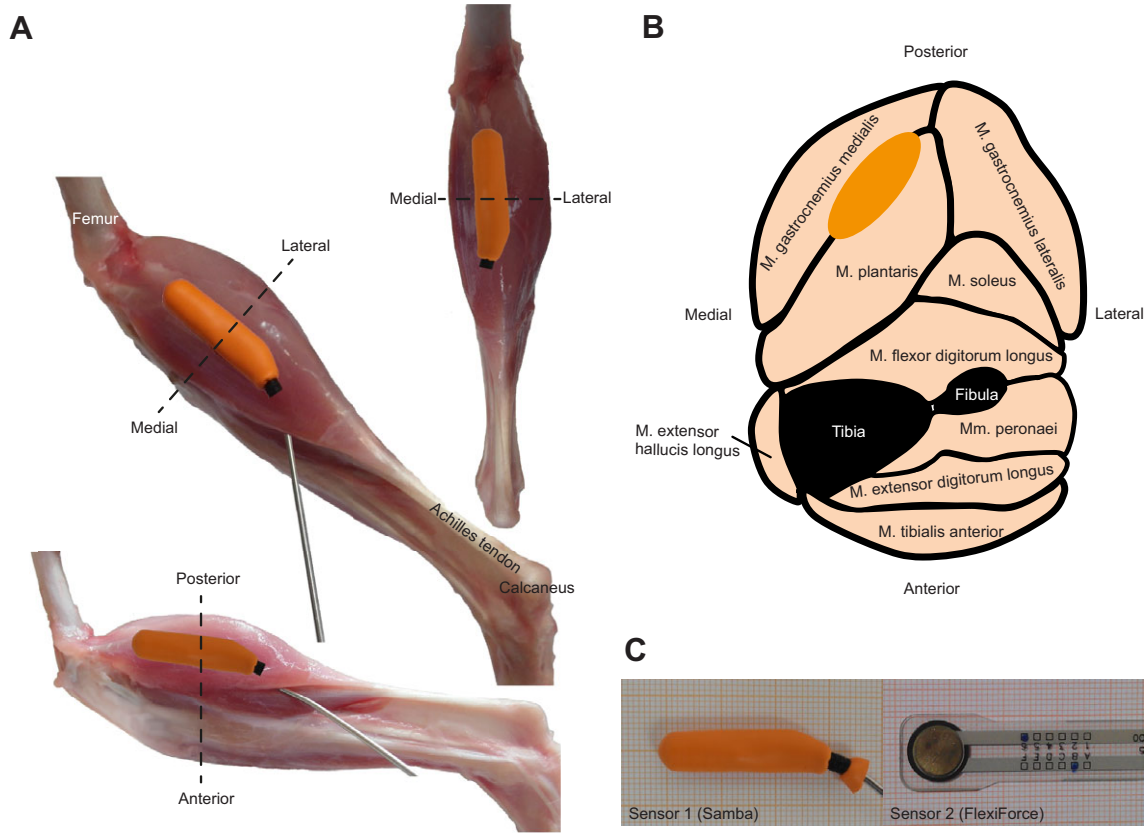

Fig. 1. Transducers for measuring the intermuscular pressure (IrMP), and their position in the calf muscles of *Oryctolagus cuniculus* during the experiments. (A) Visualisation of the measurement position in a dissected right shank of *O. cuniculus*. For the experiments, one of the two transducers shown in C was inserted from medial as centrally as possible between the contact area of M. gastrocnemius medialis and M. plantaris. The black dashed lines mark the transversal cross-section of the limb shown in B. (C) One transducer (left; Sensor 1) consisted of a water-filled rubber balloon fixed to an irrigation cannula and connected with the Samba system. The second device (right; Sensor 2) was the FlexiForce sensor equipped with thin brass discs on the upper and lower side. Both sensors were photographed on scale paper (smallest squares: 1 mm×1 mm).

length and all muscle length data were given corresponding to it. Data are presented as means±s.d.

RESULTS

The examination of the curve progressions of muscle force and IrMP revealed almost identical time courses (Fig. 2). For the trials (n=55) that were included in the determination of the force–length and pressure–length relationships, we found an average correlation of 0.966±0.066 between F and IrMP.

Isometric (constant MTU length) forces generated by the muscle package (GAS, SOL and PLA) increased almost linearly with increasing muscle length (note, l=0 is related to the length at which F is zero) up to 12.4±1.3 mm (Fig. 3A and Table 1). The corresponding ascending limb of the force–length relationship was approximated by a linear function (r^2>0.99; Table 1). Maximum isometric force (F_{im}) averaged at 204.6±40.0 N and was reached at a muscle length of 14.8±1.5 mm (Table 1).

Similar to F, IrMP increased linearly with l in the ascending limb of the force–length curve, too. From zero muscle length up to a muscle length of 11.1±2.8 mm, we found a high degree of linearity (r^2>0.98) between both parameters (Table 1). IrMP ranged between 130 and 650 mbar (Fig. 3B and Table 1). At optimum muscle

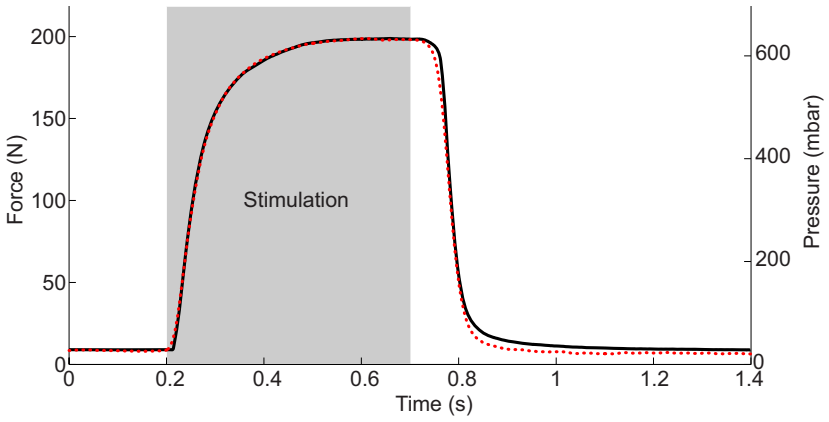

Fig. 2. Exemplary time courses of muscle force and intermuscular pressure during an isometric contraction. Total force of the calf muscles and corresponding pressure between M. gastrocnemius medialis and M. plantaris are shown as a black curve and red dotted line, respectively. The fact that both trajectories progress almost identically is further supported by a high correlation coefficient (r=0.9995). Muscle activation interval (0.5 s at 130 Hz) is illustrated by a grey bar. Data originate from an experiment on CA5 at the optimal muscle length (l_{opt}=12.9 mm; Table 1).

Journal of Experimental Biology

Journal of Experimental Biology (2016) 219, 2311-2319 doi:10.1242/jeb.135566

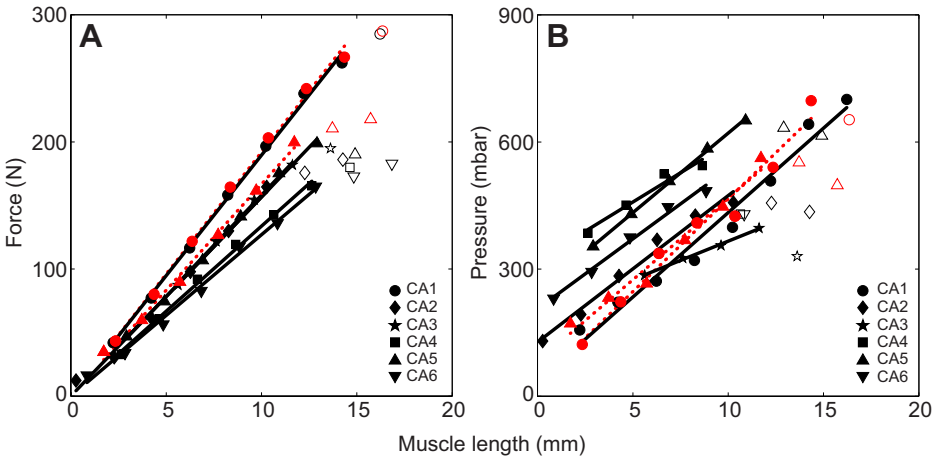

Fig. 3. Force–length and pressure–length relationship in the calf muscles. (A) The force–length relationship (up to F_{im}) of the ascending limb. (B) Corresponding intermuscular pressure between M. gastrocnemius medialis and M. plantaris depending on muscle length. In both diagrams, values belonging to one subject are depicted by the same marker form (N=6, see key). Readings that were considered for the illustrated linear regression analyses are indicated by filled markers. Values that were excluded from the linear fit are represented by unfilled symbols. The linear equations are given in Table 1. Measurement series in which the Samba fibre-optic pressure transducer (Sensor 1) and the FlexiForce sensor (Sensor 2) were used are shown in black and red colour, respectively.

lengths (plateau region of the force–length relationship), pressures up to 700 mbar were recorded (Table 1). The mean slope of the pressure–length curve measured using Sensor 1 was 31.8±7.9 mbar mm^{-1} featuring a mean intercept of 186.5±98.3 mbar (Table 1). Owing to linear dependencies of force and pressure on muscle length, the force–pressure relationship also exhibited a linear characteristic (r^2>0.94; data not shown).

Comparative measurements with Sensor 2 revealed similar results for CA1 and CA5 (red symbols in Fig. 3). This applies in particular to the slopes of the pressure–length relationships. Nevertheless, the axis intercepts of these curves were on average larger and more variable in the experiments using Sensor 1 (Fig. 3 and Table 1).

Changing muscle force at constant muscle length by variations in stimulation frequency resulted in high correlations between F and IrMP (r>0.94; Table 2 and Fig. 4) for all subjects. Muscle force and IrMP increased from about 36 N to about 179 N and 68 mbar to 461 mbar, respectively.

DISCUSSION

IrMP correlates with muscle force

The objective of the present study was to examine the relationship between muscle force and IrMP by performing two different types of experiments: (1) we varied F by changing l, owing to the fact that muscle force is length dependent (Blix, 1894; Gordon et al., 1966; Rode et al., 2009b); and (2) F was varied by changing muscle force via the stimulation frequency because F depends on f (Roszek et al., 1994). Both experimental settings demonstrated a highly linear relationship between F and IrMP (see Results). Furthermore, both parameters showed almost identical time courses in all experiments (see, for example, Fig. 2). Consequently, IrMP depends on muscle force but not on the length of the MTU.

The following circumstances might explain these findings. (1) Throughout their entire length, the GAS and PLA of *O. cuniculus* run parallel to each other and have their origin in close proximity at the distal end of the femur. Furthermore, the tendons of both muscles proceed side by side up to the calcaneus (Fig. 1A). The point of force application was even the same, owing to the clamping connection with the muscle lever. (2) As known from earlier studies, calf muscles show substantial changes in shape during isometric and dynamic contractions (Böl et al., 2013, 2015). (3) Also, muscle hardness, i.e. the resistance offered by the muscle against perpendicular pressure, considerably increases with rising force during contraction (Horikawa et al., 1993; Murayama et al., 2005, 2012). On the basis of these facts, the following simple explanatory approach is suggested (Fig. 5). IrMP at the contact area between two muscles rises during contraction, owing to considerably increased transverse forces. This in turn results from the fact that muscle-generated forces are not acting along the direct line between origin and insertion. In addition, muscle deformation and increased hardness further strengthen this effect. A similar argument has been previously used by several authors in order to explain variations in IaMP through changes in the curvature of muscle fibres and tendinous sheets during contraction (Hill, 1948; Heukelom et al., 1979; Otten, 1988; van Leeuwen and Spoor, 1992).

Influence of serial elasticity

As can be seen in Fig. 1, series elastic structures (e.g. tendons) take a considerable proportion of the MTU length in the calf musculature. A recent study on the same species as used here determined that – owing to the compliance of these tissues – there were elongations of about 5 mm when the muscles developed maximum forces (Siebert et al., 2015). Accordingly, the muscle-belly length must decrease at the same time because muscle fascicles are shortening. Therefore, in our experiments, the muscles did not operate isometrically with regard to the fibres. Similar experiments on the GAS of cats revealed that the maximal shortening of muscle fibres was 28% (Griffiths, 1991). Additionally, the same study identified a nearly identical shape of shortening–time and the force–time traces. It is therefore impossible to mechanistically decouple force and shortening over the time course of isometric contractions performed on muscle–tendon complexes with constant length. In order to gain a better understanding of this issue, one future approach should be to

Table 2. Correlation between intermuscular pressure (IrMP) and muscle force at equal muscle lengths

	CA1	CA2	CA3	CA4	CA5	CA6	Mean	s.d.
Symbol	●	◆	★	■	▲	▼		
l_{PF} (mm)	14.4	10.3	11.6	6.6	15.7	14.8	12.2	3.4
r	0.982	1.000	0.974	0.997	0.987	0.940	0.980	0.022

Muscle force was varied by stimulation frequencies from 20 to 130 Hz.
l_{PF} is the constant muscle length for experiments with different stimulation frequencies.

Journal of Experimental Biology (2016) 219, 2311-2319 doi:10.1242/jeb.135566

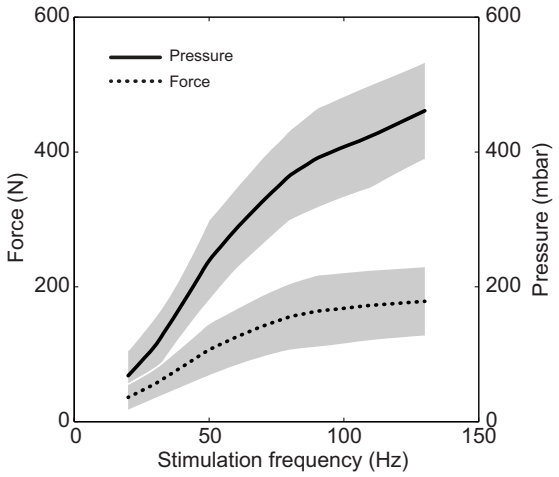

Fig. 4. Muscle force and IrMP depending on muscle activation. Mean values are shown as black lines (solid: IrMP; dotted: muscle force) surrounded by grey areas visualising the s.d. (N=6). The similarity between both curves (Table 2) is confirmed by a high average correlation coefficient (r=0.98).

perform isotonic contractions where force can be kept constant, but shortening could be varied by changing the stimulus duration.

However, stimulus duration was chosen so that a tetanic force plateau was reached in every trial (see Fig. 2). At least during this time period, a truly isometric contraction of the muscle fibres can be assumed. Nevertheless, the mentioned changes in muscle shape, which are a major circumstance for our explanatory model (Fig. 5), are only possible under the condition of muscle-fibre (or muscle-belly) shortening.

Serial elasticity is also relevant in the measurement series in which the stimulation frequency was varied. One advantage of assessing this data set from the ascending limb of the force–length relationship is that, as stimulation frequency increased, the muscle fibres likely shortened and thus moved to a lower force region of their force–length relationship. However, the total force and IrMP increased and, consequently, the increases in IrMP were caused despite, and not because of, the force–length properties of the muscle fibres.

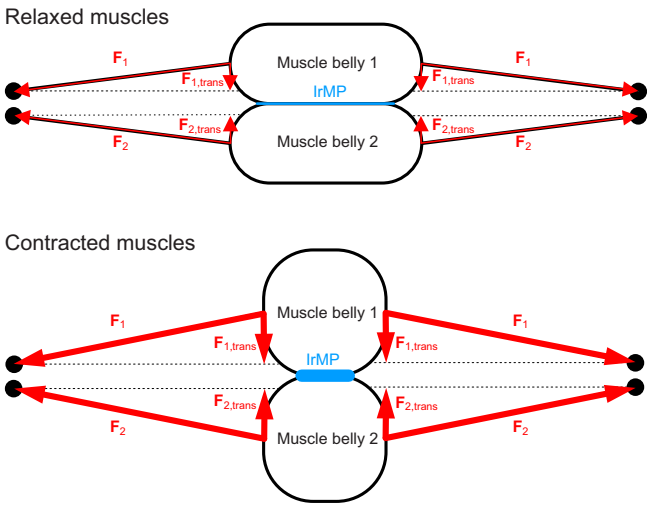

Fig. 5. Schematic illustration of the pressure increase between synergistic muscles during an isometric contraction. In the relaxed situation (upper panel), intermuscular pressure (IrMP; thin blue line) is low because transverse forces ($\mathbf{F}_{1,trans}$ and $\mathbf{F}_{2,trans}$) are small. With growing muscle forces ($\mathbf{F}_1$ and $\mathbf{F}_2$) during contraction (bottom panel), transverse forces also increase. Consequently, both muscles are pressed against each other, resulting in a rise in IrMP (thick blue line). Changes in muscle form (increase in muscle thickness) further enhance transversal forces owing to the fact that the vertical distance between the muscle–tendon connection and the line of action (dotted line) increases. The simultaneous increase in muscle hardness leads to direct transmission of these forces to the contact area between both muscles, which is equivalent to an increase in IrMP. The magnitudes of force and pressure are symbolised by line width.

Comparison with literature

Until now, no measurements regarding the pressure between adjacent muscles have been published. For this reason, our results can only be compared with studies on IaMP. Interestingly, a few reports exist examining IaMP in rabbit TA (Davis et al., 2003; Ward et al., 2007; Winters et al., 2009). Under isometric conditions, this muscle produced maximum forces and corresponding peak IaMP values of about 20 N and 60 mbar, respectively. However, and as presented here, the total force produced by the calf-muscle package can be around 14 times higher (287 N; Table 1). Considering these higher muscle forces, higher peak IaMP values are to be expected as well. Lower IaMP may be further explained by the superficial localisation (Fig. 1B) of the TA and the absence of overlying muscles and, thus, transversal compression. Moreover, the lower pennation angles of TA (approximately 3 deg; Lieber and Blevins, 1989) compared with that of the calf muscles (approximately 15 deg; Siebert et al., 2015) result in lower transversal forces, which might contribute to lower IaMP.

Although reports on measurements of IaMP in the calf muscles of rabbits are lacking, studies on the lower legs of cats are available for comparison owing to existing similarities in anatomy, strength and muscle properties (Herzog et al., 1992; Young et al., 1993; Siebert et al., 2008). IaMP measured in the belly of the M. gastrocnemius medialis of cats reached maximum values around 240–400 mbar (Mazzella and Bauer, 1953; Petrofsky and Hendershot, 1984). This is in accordance with previous results for the GAS of a frog (Hill, 1948).

IaMP in human muscles can significantly exceed these values. In the SOL and GAS, for example, peak values of up to 330–500 mbar were found (Sadamoto et al., 1983; Aratow et al., 1993; Ballard et al., 1998). However, the highest pressure values were determined in the thigh musculature. During maximum isometric contraction, IaMP in the M. vastus medialis averaged at 640 mbar, whereas, in a single trial, even 1400 mbar was measured (Sylvest and Hvid, 1959).

Moreover, almost all mentioned investigations demonstrated a high correlation between IaMP and muscle force. This finding coincides with the fact that muscle hardness and longitudinal stiffness increase with force generation (Morgan, 1977; Horikawa et al., 1993; Ettema and Huijing, 1994; Murayama et al., 2005, 2012).

IrMP is in a relevant range to affect muscle function

IrMP found between GAS and PLA was about 100–700 mbar, corresponding to 1 to 7 N cm^{-2}. Application of local transversal pressures in these ranges (1.3–5.3 N cm^{-2}) induced by a plunger on rat M. gastrocnemius medialis resulted in a reduction of muscle forces by 5–13% (Siebert et al., 2014b). These results suggest that the observed IrMP between rabbit GAS and PLA can reduce the muscle force produced by both muscles during contraction. This hypothesis is supported by the measured lower (26%) muscle forces of whole muscle packages (mean≈205 N; Table 1) as compared with the sum of forces generated by isolated calf muscles (mean≈278 N; Siebert et al., 2015; mean muscle masses and cross-sectional areas were similar in both studies). However, there

may be additional reasons for the lower muscle-package forces observed in the present study. For example, muscle length of the PLA was adjusted to reach F_{im} at almost the same muscle-lever arm excursion as the GAS and SOL. For this purpose, we used the mean optimum muscle length of six single muscles determined in a previous study (Siebert et al., 2015). However, individual differences in optimum muscle lengths might lead to lower whole muscle package forces. In addition, muscle deformation might result in transversal displacement and thus in elongation of adjacent muscles. Because experiments were performed on the ascending limb and plateau region of the force–length relationship, muscle lengthening will result in constant or even increasing muscle forces. Thus, the influence of transversal compressing forces induced by neighbouring muscles on whole muscle package force should be investigated in further studies examining isolated and combined muscle forces.

Modelling the interaction between rat M. gastrocnemius medialis and a transversal load (compressing the muscle), the reduction in muscle force was explained by balancing the transversal load and performing lifting work to lift the load during muscle deformation (Siebert et al., 2014a). The basic idea of this model approach is that the mechanical work performed by the muscle fibres is equal to the energy provided to their mechanical environment. This includes the mechanical work on internal structures, e.g. tendons, passive connective tissue and the work carried out externally, e.g. deformation of surrounding tissues. Owing to differences in the transversal loading situation (local compression by a plunger versus rather global compression on large fractions of the muscle surface), muscle size, architecture and species, the transferability of these findings needs to be elucidated in the future.

Potential benefits from IrMP

If the architecture of the calf muscles would ensure that they optimally fit together in shape during contraction, i.e. without interfering with each other, IrMP should have been low. Because we determined relatively high IrMP values, this aspect does not seem to be the main criterion in the design of muscle packages. However, if a reduction in muscle force induced by IrMP exists, transverse forces induced by surrounding muscles may fulfil a specific function. Compression of muscles may contribute to stabilisation of muscle packages (e.g. during impacts in locomotion; Günther et al., 2003). Moreover, compressed muscles may act under dynamically more favourable conditions (e.g. shifting the point of muscle operation, resulting in increased work production; Siebert et al., 2014a). Furthermore, work performed transversally on adjacent muscles may be saved and released subsequently. Additionally to energy savings in parallel (Rode et al., 2009a) and series (Biewener and Roberts, 2000) elastic structures, this would provide another possibility of energy savings during locomotion, which might enhance the efficiency of cyclical locomotion. IrMP associated with transmission of transversal forces may be functionally relevant regarding, for example, stabilisation of the spine by back muscles (Morlock et al., 1999; Rupp et al., 2015). However, these questions need to be addressed in more detail in future studies.

Methodological considerations

As stated above, IrMP found between rabbit GAS and PLA was clearly higher than IaMP reported for TA of the same species during isometric contractions (Davis et al., 2003; Ward et al., 2007; Winters et al., 2009). These studies used a 360 µm diameter fibre-optic pressure sensor (Luna Innovations Inc., Blacksburg, Virginia), which was similar to Sensor 1 used in the current study. However, because the muscle is filled with a fluid, the sensor could be inserted in the muscle directly. In contrast, we used a small balloon filled with water to measure IrMP.

As reported previously, transducer movement during the measurements was an unintended side-effect with significant impact on the results (Ward et al., 2007). Although, our method minimised this effect, we refrained from determining IrMP over the whole force–length curve, but confined our analyses to the ascending limb. Nevertheless, in view of the results for the IaMP, we expect the explored relationship to be valid for the descending limb and the plateau region of the force–length relationship as well.

Because our balloon transducer intentionally covered a large proportion (2.4 cm^2) of the contact surface between GAS and PLA, the determined IrMP values represent the mean pressure between both muscles. It is also conceivable that the pressure is unevenly distributed across the surface. This can only be evaluated in detail using a much smaller sensor at multiple measuring points, or a miniature matrix pressure sensor. Considering that the clearly smaller (0.7 cm^2) Sensor 2 revealed similar results and the fact that the contact area between the GAS and PLA is very flat, we expect only small local deviations from our current results.

We determined similar slopes but different axis intercepts in the pressure–length relationships. In contrast to clearly smaller axis intercepts determined with Sensor 2, we found larger and much more variable axis intercepts for Sensor 1 (Fig. 3 and Table 1). This could have geometric causes. Balloon filling was adapted by hand before each measurement series in order to avoid complete balloon squeezing at pressures up to 1 bar. As a matter of course, slightly different filling volumes can affect the position of the muscles to each other, i.e. spreading them apart. In accordance with our explanatory approach (Fig. 5), a bigger sensor height would increase the distance between both muscles, i.e. the distance between the muscle–tendon connection and the line of action. Consequently, transverse forces would be increased and IrMP would be on a higher level at the same time. Besides this context, a certain variability is even to be expected owing to the fact that muscle hardness in maximum isometric contractions is variable as well (Murayama et al., 2012). Muscle hardness in turn is strongly affected by IaMP (Steinberg and Gelbermann, 1994; Steinberg, 2005), which is more variable as compared with muscle force throughout the entire isometric length–tension relationship (Ward et al., 2007; Winters et al., 2009).

Conclusion

Finally, it can be stated that IrMP within the calf muscles of *O. cuniculus* lies in the range of IaMP measured in skeletal muscles of different vertebrates. As has been already demonstrated for IaMP, IrMP is also correlated to muscle force under isometric conditions. Additionally, there is some indication that the occurrence of IrMP affects the force development in muscle packages. Possible mechanisms of IrMP were related to transversal forces induced by deformation and thickening of synergistic muscles during isometric contraction. Results of the present study are of interest for modelling and interpreting three-dimensional muscle architectures and deformations with respect to active force generation of muscle packages.

Competing interests

The authors declare no competing or financial interests.

Author contributions

L.R., K.L. and T.S. performed experiments; L.R. analysed data and prepared figures; L.R., T.S., R.B. and M.B. designed the study, interpreted results, and edited, revised and drafted the manuscript; all authors approved the final version of manuscript.

Funding
This work was funded by the Deutsche Forschungsgemeinschaft [German Research Foundation (DFG)] under grant SI 841/3-1, 2 and BO 3091/4-1, 2 to T.S. and M.B., respectively.

References

Aratow, M., Ballard, R. E., Crenshaw, A. G., Styf, J., Watenpaugh, D. E., Kahan, N. J. and Hargens, A. R. (1993). Intramuscular pressure and electromyography as indexes of force during isokinetic exercise. *J. Appl. Physiol.* **74**, 2634-2640.
Ballard, R. E., Watenpaugh, D. E., Breit, G. A., Murthy, G., Holley, D. C. and Hargens, A. R. (1998). Leg intramuscular pressures during locomotion in humans. *J. Appl. Physiol.* **84**, 1976-1981.
Baskin, R. and Paolini, P. (1967). Volume change and pressure development in muscle during contraction. *Am. J. Physiol.* **213**, 1025-1030.
Biewener, A. A. and Roberts, T. J. (2000). Muscle and tendon contributions to force, work, and elastic energy savings: a comparative perspective. *Exerc. Sport Sci. Rev.* **28**, 99-107.
Blix, M. (1894). Die Länge und die Spannung des Muskels. *Acta Physiol.* **5**, 150-173.
Böl, M., Leichsenring, K., Weichert, C., Sturmat, M., Schenk, P., Blickhan, R. and Siebert, T. (2013). Three-dimensional surface geometries of the rabbit soleus muscle during contraction: input for biomechanical modelling and its validation. *Biomech. Model. Mechanobiol.* **12**, 1205-1220.
Böl, M., Leichsenring, K., Ernst, M., Wick, C., Blickhan, R. and Siebert, T. (2015). Novel microstructural findings in M. plantaris and their impact during active and passive loading at the macro level. *J. Mech. Behav. Biomed. Mater.* **51**, 25-39.
Cottler, P. S., Karpen, W. R., Morrow, D. A. and Kaufman, K. R. (2009). Performance characteristics of a new generation pressure microsensor for physiologic applications. *Ann. Biomed. Eng.* **37**, 1638-1645.
Davis, J., Kaufman, K. R. and Lieber, R. L. (2003). Correlation between active and passive isometric force and intramuscular pressure in the isolated rabbit tibialis anterior muscle. *J. Biomech.* **36**, 505-512.
Ettema, G. J. C. and Huijing, P. A. (1994). Skeletal muscle stiffness in static and dynamic contractions. *J. Biomech.* **27**, 1361-1368.
Ferguson-Pell, M., Hagisawa, S. and Bain, D. (2000). Evaluation of a sensor for low interface pressure applications. *Med. Eng. Phys.* **22**, 657-663.
Gordon, A. M., Huxley, A. F. and Julian, F. J. (1966). The variation in isometric tension with sarcomere length in vertebrate muscle fibres. *J. Physiol.* **184**, 170-192.
Griffiths, R. (1991). Shortening of muscle fibres during stretch of the active cat medial gastrocnemius muscle: the role of tendon compliance. *J. Physiol.* **436**, 219-236.
Günther, M., Sholukha, V. A., Kessler, D., Wank, V. and Blickhan, R. (2003). Dealing with skin motion and wobbling masses in inverse dynamics. *J. Mech. Med. Biol.* **3**, 309-335.
Herzog, W., Leonard, T. R., Renaud, J. M., Wallace, J., Chaki, G. and Bornemisza, S. (1992). Force-length properties and functional demands of cat gastrocnemius, soleus and plantaris muscles. *J. Biomech.* **25**, 1329-1335.
Heukelom, B., van der Stelt, A. and Diegenbach, P. C. (1979). A simple anatomical model of muscle, and the effects of internal pressure. *Bull. Math. Biol.* **41**, 791-802.
Hill, A. V. (1948). The pressure developed in muscle during contraction. *J. Physiol.* **107**, 518-526.
Horikawa, M., Ebihara, S., Sakai, F. and Akiyama, M. (1993). Non-invasive measurement method for hardness in muscular tissues. *Med. Biol. Eng. Comput.* **31**, 623-627.
Jenkyn, T. R., Koopman, B., Huijing, P., Lieber, R. L. and Kaufman, K. R. (2002). Finite element model of intramuscular pressure during isometric contraction of skeletal muscle. *Phys. Med. Biol.* **47**, 4043-4061.
Kaufman, K. R., Wavering, T., Morrow, D., Davis, J. and Lieber, R. L. (2003). Performance characteristics of a pressure microsensor. *J. Biomech.* **36**, 283-287.
Lieber, R. L. and Blevins, F. T. (1989). Skeletal muscle architecture of the rabbit hindlimb: Functional implications of muscle design. *J. Morphol.* **199**, 93-101.
Macias, B. R., D'Lima, D. D., Cutuk, A., Patil, S., Steklov, N., Neuschwander, T. B., Meuche, S., Colwell, C. W. and Hargens, A. R. (2012). Leg intramuscular pressures and in vivo knee forces during lower body positive and negative pressure treadmill exercise. *J. Appl. Physiol.* **113**, 31-38.
Mazzella, H. and Bauer, C. M. (1953). The pressure developped by skeletal muscle during contraction. *Arch. Int. Physiol.* **61**, 453-461.
McGinnis, P. M. (1999). *Biomechanics of Sport and Exercise*. Champaign, IL: Human Kinetics.
Mendez, J. and Keys, A. (1960). Density and composition of mammalian muscle. *Metabolism* **9**, 184-188.
Morgan, D. L. (1977). Separation of active and passive components of short-range stiffness of muscle. *Am. J. Physiol. Cell Physiol.* **232**, 45-49.
Morlock, M. M., Bonin, V., Hansen, I., Günther, M. and Schmitt, S. (1999). Die Rolle der Muskulatur bei bandscheibenbedingten Erkrankungen der Wirbelsäule. In *Prävention von arbeitsbedingten Gesundheitsgefahren und Erkrankungen des Stütz- und Bewegungssystems - 6. Erfurter Tage* (ed. S. Radandt, R. Grieshaber and W. Schneider), pp. 68-69. Leipzig: monade.
Murayama, M., Yoneda, T. and Kawai, S. (2005). Muscle tension dynamics of isolated frog muscle with application of perpendicular distortion. *Eur. J. Appl. Physiol.* **93**, 489-495.
Murayama, M., Watanabe, K., Kato, R., Uchiyama, T. and Yoneda, T. (2012). Association of muscle hardness with muscle tension dynamics: a physiological property. *Eur. J. Appl. Physiol.* **112**, 105-112.
Nakhostine, M., Styf, J. R., van Leuven, S., Hargens, A. R. and Gershuni, D. H. (1993). Intramuscular pressure varies with depth: the tibialis anterior muscle studied in 12 volunteers. *Acta Orthop. Scand.* **64**, 377-381.
Otten, E. (1988). Concepts and models of functional architecture in skeletal muscle. *Exerc. Sport Sci. Rev.* **16**, 89-138.
Parker, P. A., Körner, L. and Kadefors, R. (1984). Estimation of muscle force from intramuscular total pressure. *Med. Biol. Eng. Comput.* **22**, 453-457.
Petrofsky, J. S. and Hendershot, D. M. (1984). The interrelationship between blood pressure, intramuscular pressure, and isometric endurance in fast and slow twitch skeletal muscle in the cat. *Eur. J. Appl. Physiol. Occup. Physiol.* **53**, 106-111.
Rode, C., Siebert, T. and Blickhan, R. (2009a). Titin-induced force enhancement and force depression: A 'sticky-spring' mechanism in muscle contractions? *J. Theor. Biol.* **259**, 350-360.
Rode, C., Siebert, T., Herzog, W. and Blickhan, R. (2009b). The effects of parallel and series elastic components on the active cat soleus force-length relationship. *J. Mech. Med. Biol.* **9**, 105-122.
Röhrle, O., Davidson, J. B. and Pullan, A. J. (2008). Bridging scales: a three-dimensional electromechanical finite element model of skeletal muscle. *SIAM J. Sci. Comput.* **30**, 2882-2904.
Roszek, B., Baan, G. C. and Huijing, P. A. (1994). Decreasing stimulation frequency-dependent length-force characteristics of rat muscle. *J. Appl. Physiol.* **77**, 2115-2124.
Rupp, T. K., Ehlers, W., Karajan, N., Günther, M. and Schmitt, S. (2015). A forward dynamics simulation of human lumbar spine flexion predicting the load sharing of intervertebral discs, ligaments, and muscles. *Biomech. Model. Mechanobiol.* **14**, 1081-1105.
Sadamoto, T., Bonde-Petersen, F. and Suzuki, Y. (1983). Skeletal muscle tension, flow, pressure, and EMG during sustained isometric contractions in humans. *Eur. J. Appl. Physiol. Occup. Physiol.* **51**, 395-408.
Sejersted, O. M., Hargens, A. R., Kardel, K. R., Blom, P., Jensen, O. and Hermansen, L. (1984). Intramuscular fluid pressure during isometric contraction of human skeletal muscle. *J. Appl. Physiol.* **56**, 287-295.
Sezen, A. S., Rajamani, R., Morrow, D., Kaufman, K. R. and Gilbert, B. K. (2009). An ultraminiature MEMS pressure sensor with high sensitivity for measurement of intramuscular pressure (IMP) in patients with neuromuscular diseases. *J. Med. Device* **3**, e031006.
Siebert, T., Rode, C., Herzog, W., Till, O. and Blickhan, R. (2008). Nonlinearities make a difference: comparison of two common Hill-type models with real muscle. *Biol. Cybern.* **98**, 133-143.
Siebert, T., Günther, M. and Blickhan, R. (2012). A 3D-geometric model for the deformation of a transversally loaded muscle. *J. Theor. Biol.* **298**, 116-121.
Siebert, T., Till, O. and Blickhan, R. (2014a). Work partitioning of transversally loaded muscle: experimentation and simulation. *Comput. Methods Biomech. Biomed. Engin.* **17**, 217-229.
Siebert, T., Till, O., Stutzig, N., Günther, M. and Blickhan, R. (2014b). Muscle force depends on the amount of transversal muscle loading. *J. Biomech.* **47**, 1822-1828.
Siebert, T., Leichsenring, K., Rode, C., Wick, C., Stutzig, N., Schubert, H., Blickhan, R. and Böl, M. (2015). Three-dimensional muscle architecture and comprehensive dynamic properties of rabbit gastrocnemius, plantaris and soleus: input for simulation studies. *PLoS ONE* **10**, e0130985.
Siebert, T., Rode, C., Till, O., Stutzig, N. and Blickhan, R. (2016). Force reduction induced by unidirectional transversal muscle loading is independent of local pressure. *J. Biomech.* **49**, 1156-1161.
Sondergaard, S., Karason, S., Hanson, A., Nilsson, K., Hojer, S., Lundin, S. and Stenqvist, O. (2002). Direct measurement of intratracheal pressure in pediatric respiratory monitoring. *Pediatr. Res.* **51**, 339-345.
Steinberg, B. D. (2005). Evaluation of limb compartments with increased interstitial pressure. An improved noninvasive method for determining quantitative hardness. *J. Biomech.* **38**, 1629-1635.
Steinberg, B. D. and Gelbermann, R. H. (1994). Evaluation of limb compartments with suspected increased interstitial pressure: a noninvasive method for determining quantitative hardness. *Clin. Orthop. Relat. Res.* **300**, 248-253.
Styf, J. and Körner, L. (1986). Microcapillary infusion technique for measurement of intramuscular pressure during exercise. *Clin. Orthop. Relat. Res.* **207**, 253-262.
Swammerdam, J. (1737). *Biblia naturae: sive historia insectorum*. Leiden: Isaacum Severinum.
Sylvest, O. and Hvid, N. (1959). Pressure measurements in human striated muscles during contraction. *Acta Rheumatol. Scand.* **5**, 216-222.

Tohyama, O., Kohashi, M., Fukui, M. Itoh, H. (1997). A fiber-optic pressure microsensor for biomedical applications. In International Conference on Solid State Sensors and Actuators (TRANSDUCERS '97), Vol. 2, pp. 1489-1492. Chicago, IL.

van Leeuwen, J. L. and Spoor, C. W. (1992). Modelling mechanically stable muscle architectures. *Philos. Trans. R. Soc. B Biol. Sci.* **336**, 275-292.

Wakeling, J. M., Jackman, M. and Namburete, A. I. (2013). The effect of external compression on the mechanics of muscle contraction. *J. Appl. Biomech.* **29**, 360-364.

Ward, S. R., Davis, J., Kaufman, K. R. and Lieber, R. L. (2007). Relationship between muscle stress and intramuscular pressure during dynamic muscle contractions. *Muscle Nerve* **36**, 313-319.

Winters, T. M., Sepulveda, G. S., Cottler, P. S., Kaufman, K. R., Lieber, R. L. and Ward, S. R. (2009). Correlation between isometric force and intramuscular pressure in rabbit tibialis anterior muscle with an intact anterior compartment. *Muscle Nerve* **40**, 79-85.

Young, R. P., Scott, S. H. and Loeb, G. E. (1993). The distal hindlimb musculature of the cat: multiaxis moment arms at the ankle joint. *Exp. Brain Res.* **96**, 141-151.